
Cellular Structure of Halogen-Free Flame Retardant Foams Based on LDPE

S. Román-Lorza, M.A. Rodríguez-Perez*, and J.A. de Saja Sáez

Cellular Materials Laboratory (CellMat), Condensed Matter Physics Department, Science Faculty, University of Valladolid, 47011 Valladolid, Spain

ABSTRACT

Composites of LDPE/ATH (up to 70 wt.%) were foamed to create new materials with good fire retardancy properties and low weight, proving the feasibility of developing cellular structures when high levels of inorganic fillers are included. An experimental study was carried out to explore the effects of chemical composition on cellular structure as well as the effect of structure on their thermal, mechanical and combustion properties. Samples fabrication was carried out using an improved compression moulding route consisting of polymer compounding, precursor preparation and foaming under pressure. The polymer matrix consisted of low density polyethylene as well as certain amount of LLDPE-g-MAH as compatibilizer agent. The inorganic filler used was aluminium trihydroxide (ATH) ranging from 0 wt.% to 70 wt.%. Furthermore, azodicarbonamide (ADC) was used as chemical blowing agent.

Foamed samples with cell sizes below 100 microns were produced. These samples showed similar fire retardancy than their solid precursors. The compatibilization was proved indispensable to achieve a good adhesion between mineral filler and polymer and to improve the cellular structure. The increase of the amount of filler has an interesting effect on the cellular structure, going from a closed-cell (at low contents) to an open-cell (at higher contents) cellular structure.

As a result of this investigation, halogen-free flame retardant cellular materials were processed, leading to a notable reduction of material compared to the solid one and to new properties which can result in new applications.

* To whom correspondence should be addressed, email: marrod@fmc.uva.es,
Tel: +34 983 184035, Fax: +34 983 423192

©Smithers Rapra Technology, 2009

1. INTRODUCTION

In the last few years fire codes and regulations pertinent to plastics are becoming more and more stringent. Due to the increasing use of polymeric materials in our everyday live, the risk of fire has become an extremely important issue in all kind of areas such as the automotive, aeronautics or construction sectors among others. Only building materials and components that have passed certain fire tests and therefore meet fire performance requirements are used⁽¹⁻³⁾.

On the other hand, the majority of end users and materials' industries are rejecting the use of halogenated flame retardants due to their inherent toxicity and their persistence in the environment, leading to a developing halogen-free flame retardant market^(4,5).

Aluminium hydroxide (ATH) remains the largest-volume halogen-free flame retardant, due to its low cost, good fire retardancy properties and non toxic smoke. For instance, ATH is widely used in the field of flame retarded polyolefin such as polyethylene (PE)⁽⁶⁾.

To achieve an effective fire retardancy in polymers with a high heat of combustion (such as LDPE, with ~40 MJ/kg), loadings of about 60 wt.% of ATH are needed, which substantially increase the density and alter the properties of the final composite. For instance, for an ATH content of 60 wt.% in LDPE, the density increases from 0.91 g/cm³ to 1.45 g/cm³, leading to a considerably weight increase in the structures or materials in which they take part. The aim of this work is to overcome this disadvantage obtaining a new class of materials with the same fire retardancy but with a reduced density and adequate mechanical properties. This is achieved by creating a cellular structure by foaming the solid composite trying to achieve high cell densities, small average cell sizes, getting closer to which is considered as microcellular structures, with cell diameters averaging 100 microns or less⁽⁷⁾.

Foaming with such high loading levels of inorganic fillers and with cells sizes below 100 μm, is a challenge that has not a specific presence in the open literature. Various authors have studied the role of small quantities of fillers⁽⁸⁻¹⁰⁾ (such as calcium carbonate, silica particles, nanofillers, fibres or metallic particles) because they offer not only rigidity of the solid portion of a foamed product, but also because they can be used as nucleating sites for generating a large number of small foam bubbles⁽¹¹⁾. Almost always crosslinking agents are included in polyolefins in order to improve the mechanical properties and chemical resistance as well as to bear the extensional force in the cell growth during foaming⁽¹²⁾. In this study no crosslinking agents were used, in order to create a "green" material with superior properties and easy to recycle. Particle

size and dispersion, the surface state and filler type, as well as the final density, influence the foam microstructure and its mechanical behaviour. Eventually, filler addition is a supplementary difficulty both for the processing and the modelling of composite foam behaviour, because it can lead to an embrittlement of the cell walls and therefore favour their rupture instead of their deformation at the time of bubble growth⁽¹³⁾.

As for the mechanical properties of these materials, the reinforcement level of the foam will depend on the interaction between the filler and the polymer matrix. The nonpolar nature of polyolefin makes them incompatible with hydrophilic fillers, which in turns gives a poor adhesion between the filler surface and the polymer matrix. To this end, coupling agents must be used in order to obtain a good compatibilization. The most commonly used polymeric compatibilizers include acrylic acid functionalized polypropylene and polyethylene (PP-g-AA, PE-g-AA), maleic anhydride functionalized polypropylene, polyethylene and ethylene-propylene rubber (PP-g-MAH, PE-g-MAH, EPR-g-MAH)⁽¹⁴⁻¹⁶⁾. Hippel *et al.*⁽¹⁷⁾ have proved that the adhesion of PE/ATH composites are dramatically increased by compatibilization, reflected in an improvement in both stiffness and toughness. They have also checked that the fire retardant properties are preserved when polymeric compatibilizers are used as adhesion promoters. Several studies have analyzed both the improvement in the mechanical properties and the preservation of the flammability behaviour in these kinds of blends when compatibilizers are used, making evident that they are indispensable^(18,19). In this work, a LLDPE-g-MAH has been used as compatibilizer agent.

Solid and cellular polymers differ in their fire behaviour, due to the two-phase nature of the polymeric foams, which increases surface area. Furthermore, the cellular structure also plays an important role in the fire behaviour of these materials, as an open cellular structure can promote the transport of combustible gases through the open channels of the composite matrix, while polymeric foams with mainly closed cells show a lower permeability for gases⁽¹¹⁾. Through the achievement of a microcellular structure our objective is to approach the flammability of these composite foams to that of the solid materials from which they are made.

The aim of this work is, therefore, producing LDPE/ATH cellular materials performing a complete study with regard to their mechanical, thermal and combustion properties according to their cellular structure. The final purpose is meeting all the requirements of the new fire concerning standards and at the same time reaching new advantages in the usual applications of halogen free flame retardant materials such as a decrease of weight and amount of material needed in end-products.

2. EXPERIMENTAL

2.1 Materials

The raw materials used for the experiments were:

- Low density polyethylene LDPE 2404AN00, was supplied by Sabic, with MFI=4.2 g/10 min (2.16 kg; 190 °C).
- Aluminium hydroxide with 99.7% purity Apyral® 24, was supplied by Nabaltec, with an average particle size of 8 µm and a corresponding surface area of 2.5 m²/g.
- Fusabond MB226 DE, a linear low density polyethylene was supplied by DuPont, with a high MAH graft level (0.9%), and a MFI=1.5 g/10 min (2.16 kg;190 °C), was used as compatibilizer.
- Azodicarbonamide (ADC) Unifoam AZ VI-50, used as blowing agent, with an average particle size of 10 µm, was supplied by Hebrón, S.A.
- Zinc oxide Silox Active grade provided by Safin Alcan Spain was used as ADC activator.
- Irganox 1010, was supplied by Ciba, was used as phenolic antioxidant.

2.2 Sample Preparation

Foaming was carried out by an improved compression moulding technique⁽²⁰⁾ consisting of polymer compounding, precursor preparation and foaming under pressure.

Table 1 shows the polymer/ATH proportions for all the samples with their respective melt flow index (MFI). Notice that one sample, PE50-10, was prepared with a higher level of blowing agent, 10 wt.% of azodicarbonamide, contrasting with the other samples with just 1 wt.% of azodicarbonamide, and other one, PE40-1s, was prepared without the compatibilizing agent in order to see the differences in structure and properties that the absence of the coupling agent introduces. Blends were prepared by mixing the compounds using a Haake Rheodrive 5000 co-rotating twin-screw mixer. Typical screw speed was 10 rpm and the temperature selected was 130 °C, enough for the polymer to melt, but not so high for the blowing agent to decompose leading to a premature foaming. After that, the blends were turned into pellets.

Table 1. Composition (in weight percentage) of the samples studied along the article, together with their respective MFI

Samples\Composition (wt. %)	ATH	LDPE	LLDPE-MAH	ADC	Zinc Oxide	Antioxidant	MFI (g/10 min) (130 °C; 10 kg)
PE0-1	0	94.75	4	1	0.04	0.21	6.9
PE20-1	20	74.75	4	1	0.04	0.21	5.2
PE40-1	40	54.75	4	1	0.04	0.21	3.3
PE40-1s	40	58.75	0	1	0.04	0.21	5.2
PE50-1	50	44.75	4	1	0.04	0.21	2.1
PE50-10	50	35.75	4	10	0.04	0.21	0.9
PE60-1	60	34.75	4	1	0.04	0.21	1.1
PE70-1	70	24.75	4	1	0.04	0.21	0.8

The processed composite pellets were placed into a steel mould in order to obtain cylinders of 20 mm nominal diameter and 15 mm high. Talc from Luzenac (grade A-10) was used as releasing agent. The samples were compression-moulded at 130 °C and 80 MPa in a Mega KCK-30A press. This process allows reducing the amount of trapped gas in the precursor material. Finally, the precursor was cooled down under pressure to a temperature of 40 °C. The produced precursors were transferred to desiccators and stored until foaming. These precursors are expected to have the nominal density of the final blend. This density was achieved for all the samples with an accuracy of ± 0.05 g/cm³. In addition, samples were compression-moulded for LOI tests with dimensions of 50×20×5 mm and the same conditions of temperature and pressure.

In this work an improved compression moulding route was used. This technique differs with the conventional compression moulding process over the final step of foaming. The precursor material is introduced in a mould and heated to temperatures high enough to decompose the blowing agent. During this heating process high pressure is applied to the precursor using a heavy press. Once the gas has been created the pressure is reduced allowing the foam to expand, but instead of allowing the foam to freely expand at atmospheric pressure, the foam grows under pressure. In this way, density is controlled by the design of the mould, making the expansion ratio independent on the formulation. The description of the used procedure is as follows:

The precursor material was introduced in a specific mould designed for foaming, so that the final density is controlled by the displacement of a piston; talc was also used as releasing agent. Foaming was carried out in a one-step process with a three step temperature programme, with temperatures 60-120-170 °C measured with a thermocouple close to the base of the sample. Up to 60 °C temperature was increased at a rate of 0.4 °C/s from room temperature with an applied pressure of 8 MPa (**Figure 1**), this pressure was applied using a piston entering the mould. The sample was kept in this condition (60 °C, 8 MPa) time enough to reach a homogeneous temperature distribution in the mould and the precursor. In a second phase temperature was increased from 60 °C to 120 °C at a rate of 0.4 °C/s with an initial applied pressure of 8 MPa (**Figure 1**). An increase in pressure was detected in this temperature interval, which was due to the increase in volume of the molten polymer. In the final phase, temperature was increased up to 170 °C enough for the blowing agent to decompose. This last change in temperature leads also to an increase in pressure due to the release of gas generated by the decomposition of the blowing agent, as it can be observed in **Figure 1**, where both temperature of the sample and pressure applied is showed for a generic foaming process. Once the entire blowing agent was produced, the pressure generated by the gas was reduced, allowing the foam to grow. Expansion ratio (ER) (i.e. density) was controlled

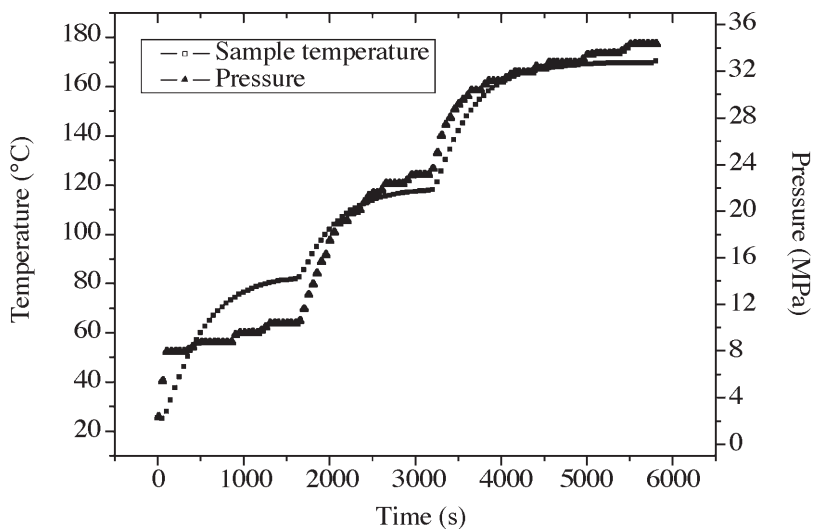


Figure 1. Temperature and pressure curves for a generic sample during the foaming process

by the displacement of the piston, the foam did not jump from the mould, it was contained on it during the whole process. A relative density (density of the foam/density of the solid) of 0.55 (i.e. expansion ratio was 1.8) was achieved in the foam expansion. Cylindrical samples of 20 mm in diameter and 25 mm in high were fabricated. The details of this foaming procedure have been published previously⁽²⁰⁾.

2.3 Analysis of the Samples

To obtain information about the influence of the filler on the molten-state of the filled polymer, measures of the melt flow index (MFI) were taken with a temperature of 130 °C and a weight of 10 kg in a ATS-FAAR Twelvindex according to the ISO standard 1133. The maximum measuring accuracy is ± 0.1 g/10 min.

Density measurements were performed by Archimedes principle using the density determination kit for the AT261 Mettler balance. Each sample was tested three times to obtain the average values of the density. The standard deviation of these measurements was $\pm 1\%$.

The morphology of the fractured surfaces of the specimens and their cellular structure was investigated with a JEOLJSM-820 scanning electron microscope (SEM). The specimens were fractured after cooling in liquid nitrogen, and then the fractured surfaces were sputter-coated with gold under argon. The electron micrographs were taken using an acceleration voltage of 5.0 kV.

The percentage of open cells was measured with a Eijkelkamp 08.06 Langer air pycnometer according to ASTM D2856-94. A total of 15 samples have been measured. The average sample volume was 6 cm³. The samples characterized, as they were cut from the original cylinders, did not present outward skin on the bases.

To calculate the pore interconnection grade (C) the following equation was used according to the ASTM normative:

$$C = \frac{V_{pyc} - V_{sample}}{V_{sample} \cdot p}$$

where the geometrical volume, V_{sample} -calculated from the dimensions of the specimen- is subtracted from the total volume measured with the pycnometer, V_{pyc} , and divided by the volume of air contained in the sample ($V_{sample} \cdot p$), i.e. the product of the sample volume and porosity.

Thermal decomposition was studied by means of a thermogravimetric analysis (TGA) Mettler Toledo TGA/SDTA851 /LF/1100 under air (thermo-oxidative conditions). The weights of the samples were approximately 10 mg and the experiments were performed between 50 °C and 850 °C. The rate of heating was 20 °C/min.

Both foamed and solid samples were conditioned at 23 °C and 50% relative humidity for 48 hours before testing the mechanical properties. Compression properties were characterized with an Instron 5500R6025 universal testing machine with a test speed of 1 mm/min and according to the standard ISO 604.

A bomb calorimeter was used to measure the combustion heat values of the samples. The measurements were made according to the standard ISO 1716 in a PARR Oxygem Bomb Calorimeter 1341EE; LOI measurements were carried out in an Oxygen Index test equipment provided by Fire Testing Technology Ltd according to the standard ASTM D2863.

A detailed description of the procedures followed to characterise these type of foamed materials have been published elsewhere⁽²¹⁻²⁵⁾.

3. RESULTS AND DISCUSSION

3.1 Structural Characterization and Cellular Structure

Firstly, by means of scanning electronic microscopy (SEM), a characterization not only of their cellular structure but also of the matrix polymer morphology was carried out. The adhesion between the mineral filler and the polymer matrix is fundamental for subsequent properties, as will be shown later, so SEM micrographs were carried out for a compatibilized and an uncompatibilized sample (**Figures 2a** and **2b**) in order to see the differences that the presence of the coupling agent introduces. It can be seen that the sample without compatibilizer shows a clear gap between ATH and polymeric matrix, whereas the compatibilized sample presents an excellent adhesion between the FR mineral and polymer, exhibiting a smoother surface. This close union is fundamental in order to obtain an improved cellular structure and mechanical behaviour, as will be seen below. All samples including the compatibilizing agent in the formulation showed an excellent adhesion between filler and polymer, even after the foaming process.

A change in the cellular structure has been observed as the loading levels are increased in the LDPE matrix, as it can be seen in **Figure 3**, where samples of 0-20-40-60 wt.% of ATH are displayed.

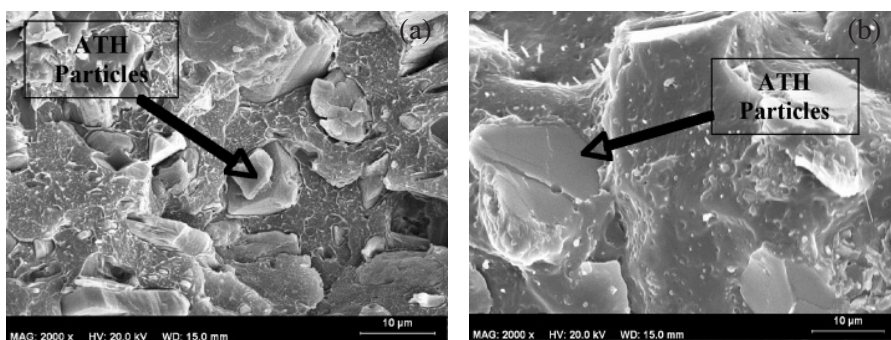


Figure 2a and 2b. SEM micrographs of the interface polymer-mineral filler between uncompatibilized samples (LDPE/ATH) (Figure a) and compatibilized samples (LDPE/LLDPE-g-MAH/ATH) (Figure b)

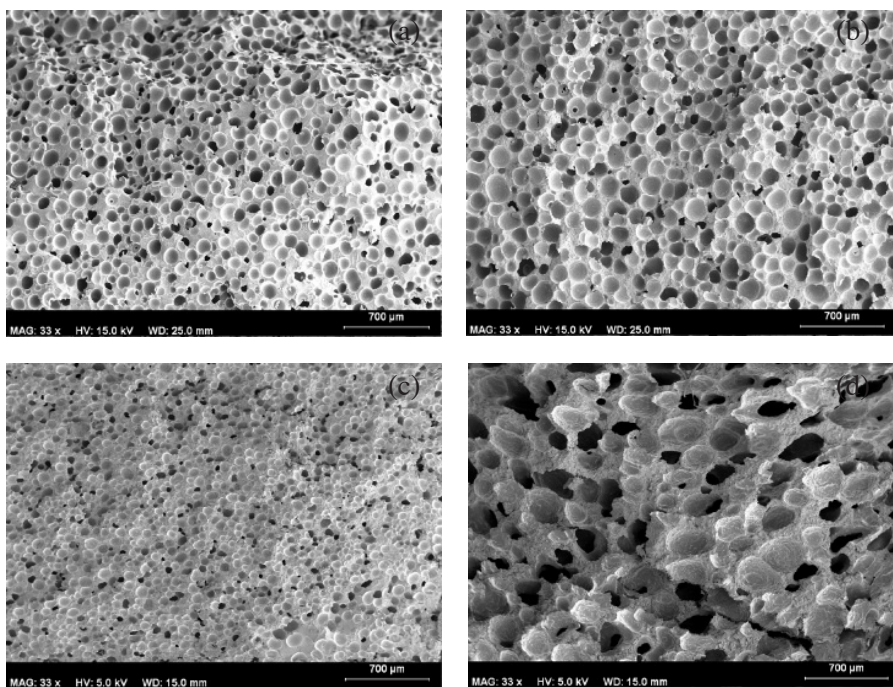


Figure 3. SEM micrographs showing the cellular structure in samples (a) PE0-1, (b) PE20-1, (c) PE40-1 and (d) PE60-1

A closed-cell cellular structure with a high degree of isotropy and homogeneity characterize most of the produced materials. Cell size also changes as the loading levels are increased, pointing out that the ATH content plays a role in the foaming behaviour of these materials.

Figure 4 shows the pattern that follows the average cell size as the loading levels are increased, reaching the lower cell size (60 μm) for those samples with 40 wt.% ATH levels, which in turn means that cells below 100 μm has been achieved.

Moreover, up to 40 wt.% loading levels the foamed samples present mainly a close cellular structure, whereas those with 60 wt.% levels of ATH present a substantial increase of interconnected cells. These results are supported by the vacuum air pycnometry measurements, as it can be seen in **Figure 5**. This figure shows the open-cell content in the foamed samples plotted against the amount of ATH. Up to 40 wt.% loading levels the open-cell content remains almost constant (around 20%), increasing with a steep slope in samples with 60 wt.% of ATH (value near 85%). Notice that this behaviour follows the same trend that the average cell size.

This result may occur because as the amount of polymer decreases the melt strength of the compound in the foaming process also decreases, leading to a different cellular structure. The structural inhomogeneity consisting of mineral particles and the molten polymer would promote cell opening in those parts

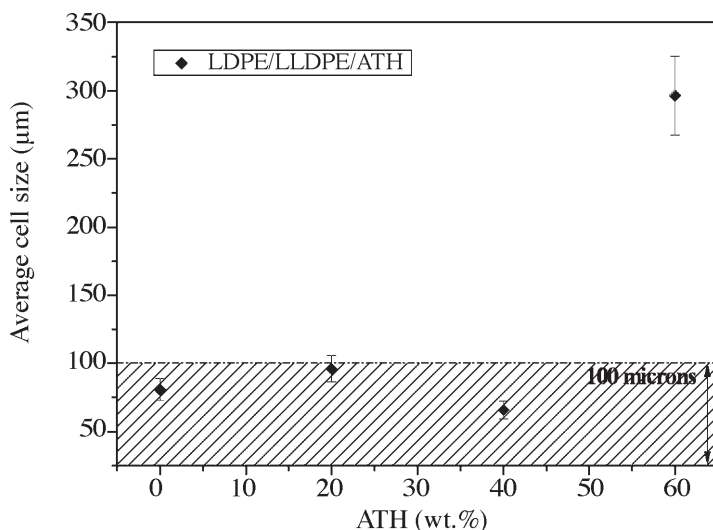


Figure 4. Average Cell Size against ATH loading level

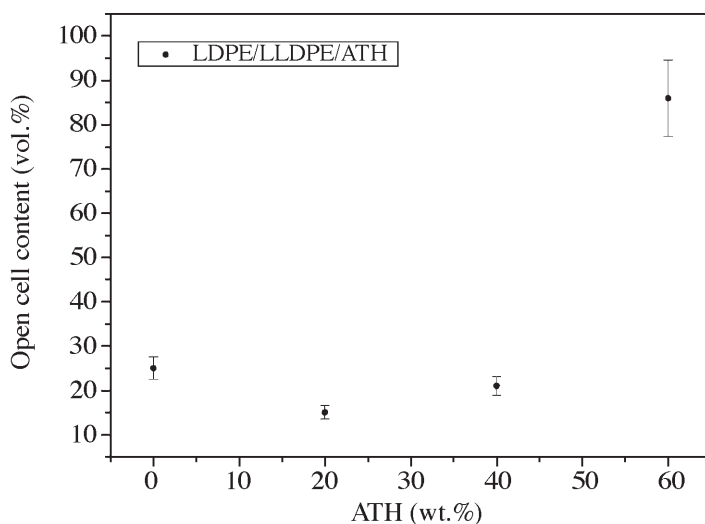


Figure 5. Effect of the loading level of ATH on the open-cell content for PE/ATH foams

where the cell walls narrow during cell growth to create interconnections between cells, while mineral particles would hold the overall structure instead of allowing the cells to completely coalesce with each other²⁶. In order to clearly observe this change in the cellular structure as the loading levels are increased from a close-cell to an open-cell cellular structure, **Figure 6** shows the cellular structure for samples PE50-1, PE60-1 and PE70-1.

While samples with 50 wt.% of ATH present mainly a close-cell cellular structure, samples with 60 wt.% are partially interconnected, as it has been proved by means of the vacuum air pycnometry measurements. But it is the change from 60 wt.% to 70 wt.% of mineral filler in the samples which turns the cellular structure into a totally interconnected one, as it can be observed in **Figure 6c**.

Another effect which is discussed herein is how the content of blowing agent affects to the cellular structure. To this end, samples with 1 wt.% and 10 wt.% are compared in **Figure 7**, where micrographs of PE50-1 and PE50-10 are displayed. It can be seen that as well as increasing the loading level of ATH leads to an open-cell cellular structure, the same effect is observed when passing from 1 wt.% to 10 wt.% of azodicarbonamide. In this case, the excess of gas generated by the decomposition of the blowing agent leads to an interconnected-cell cellular structure, with higher average cell size and important coalescence effects.

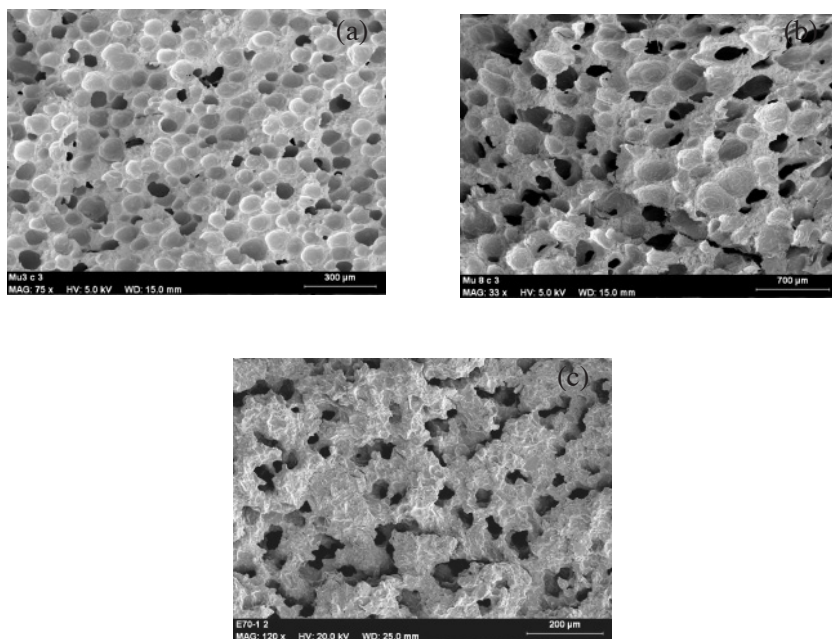


Figure 6. Changes in the cellular structure from a close-cell to an open-cell one as the loading levels are increased from (a) 50 wt.% and (b) 60 wt.% of ATH to (c) 70 wt. %

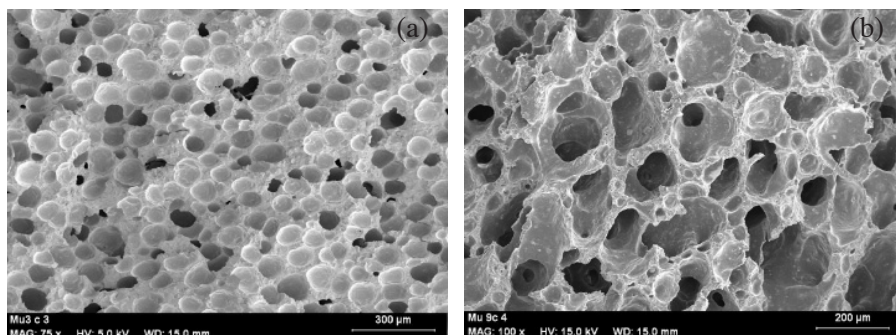


Figure 7. Changes in the cellular structure when varying the amount of blowing agent from (a) 1 wt.% to (b) 10 wt.% of ADC

3.2 Mechanical Properties

Mechanical properties of both foamed and solid samples have been measured by means of compression tests. As it was mentioned previously the relative density of foamed samples is around 0.55. The mechanical properties of materials without a coupling agent were also considered.

Tables 2 and 3 present the obtained values for Young modulus and yield strength both for the precursors and the foamed samples. It must be noticed that the values for the precursors include the presence of the blowing agent in the blends, leading to higher values than those of the same blends without the azodicarbonamide.

Table 2. Mechanical properties of the precursors as the loading level is increased. This table presents values for Young modulus and yield strength for the solid samples

Precursors	Density (g/cm ³)	Young Modulus (MPa)	Yield Strength (MPa)
PE0-1	0.9	285.8	9.2
PE20-1	1.04	339.1	11.4
PE40-1	1.22	414.1	11.9
PE40-1s	1.23	387.0	11.0
PE60-1	1.45	759.1	17.0

Table 3. Mechanical properties of the foamed samples as the loading level is increased. This table presents values for Young modulus and yield strength

Foamed Samples	Relative Density	Young Modulus (MPa)	Yield Strength (MPa)
PE0-1	0.56	28.5	1.9
PE20-1	0.55	71.8	2.8
PE40-1	0.58	113.6	3.0
PE40-1s	0.56	111.3	2.8
PE60-1	0.59	268.1	6.2

As expected, Young modulus and yield strength values increase as the amount of ATH increases. Samples with 40 wt.% of ATH and without the coupling agent present lower values than those that include this compatibilizer in their formulation. These results are obtained both for solid and foamed samples.

It should also be noted that we found the more important difference between solid and foamed samples in those without a coupling agent, proving that compatibilizing is necessary in order to improve mechanical properties due to an improved interfacial adhesion between filler and polymer.

Figure 8 shows how the effect of increasing ATH percentage leads to a Young modulus gain, as well as the yield strength is higher.

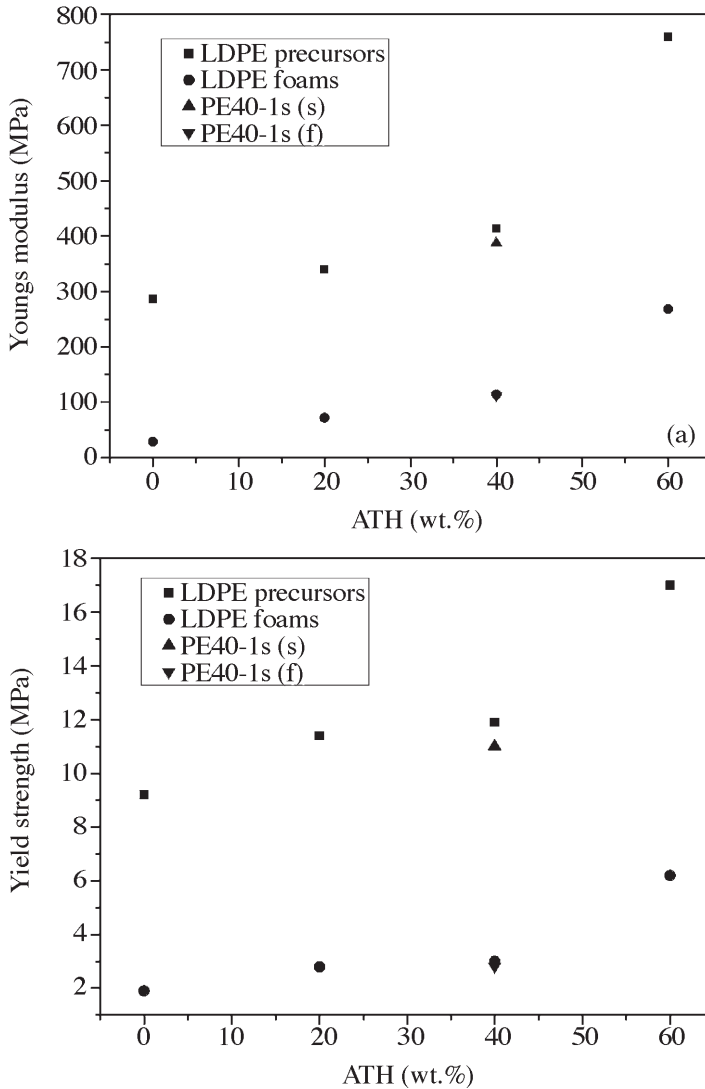


Figure 8. (a) Young's modulus and (b) yield strength vs. loading level of ATH both for solid and foamed samples. Samples without compatibilizer are also presented (PE40-1s (solid) ▲, PE40-1s (foamed) ▼)

Reducing the material's density by foaming around 50% has the effect of a Young modulus reduction of 65% for PE60-1, the highest loading level, and this difference is increased as the loading level is reduced, with its maximum for PE0-1, with a 90% difference between the foamed and the solid sample. It can be pointed out therefore that an increase in the ATH content in foamed samples approaches the behaviour to that of the corresponding solid samples.

For those samples without compatibilizer, PE40-1s, the mechanical parameters measured are reduced with regard to the correspondent compatibilized samples (**Tables 2 and 3**). As it was explained, this effect can be caused due to a lack of cohesion between the polymeric matrix and mineral particles of aluminium hydroxide.

3.3 Thermal Stability (TGA/DTG)

Thermogravimetric analysis has been carried out under air, in order to discuss the thermal stability of the foamed samples as the loading levels of aluminium hydroxide have been increased in their thermo-oxidative pattern. It has also been evaluated the differences in the decomposition profile of the foamed and solid samples.

Aluminium hydroxide decomposes endothermically in a single step between 190-350 °C with a mass loss of 35%. On the other hand, the thermo-oxidative degradation of unfilled LDPE takes place in a single step occurring in the 390-480 °C temperature range, attributed to the degradation of the hydrocarbon chains.

As can be observed in the TGA plots depicted in **Figure 9**, the onset temperature of filled samples started at lower temperatures. This behaviour is assigned to the ATH endothermic decomposition whose onset breakdown temperature is 190 °C.

In the derivative thermogravimetric curves (DTG) depicted in **Figure 9**, a first peak around 300 °C was observed occurring only in filled samples. This peak corresponds with the mass change caused by the aluminium hydroxide decomposition. Moreover, the filled LDPE blends increased thermal stability by retarding the hydrocarbon backbone degradation. This delay is made evident since the hydrocarbon backbone degradation peak temperature varies from 448 °C in PE0-1 to 469 °C in PE40-1, showing the PE60-1 sample a constant slope with a low peak at 486 °C.

In order to analyse the cellular structure contribution to the combustion behaviour, it is interesting to check if there are any differences in the decomposition

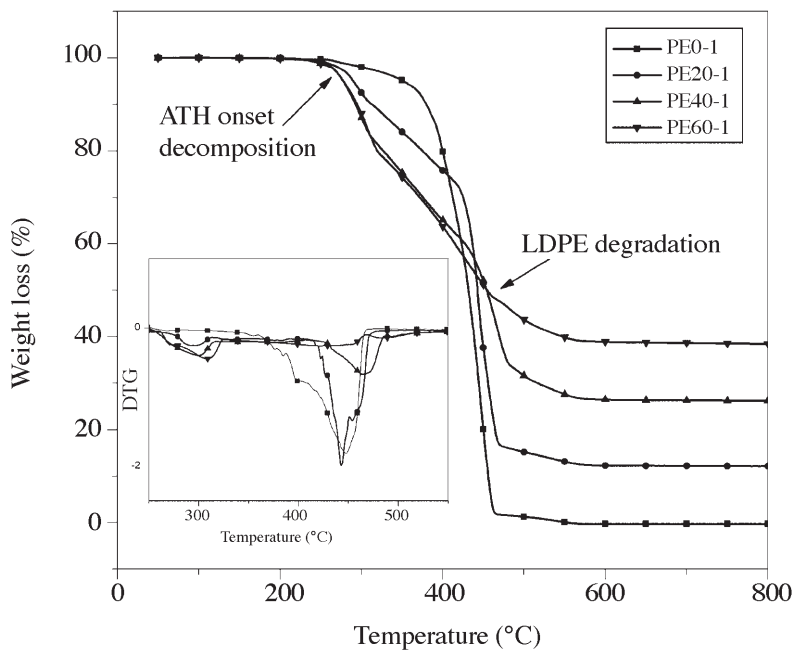


Figure 9. Thermogravimetric and their derivative (TGA/DTG) curves for foamed samples

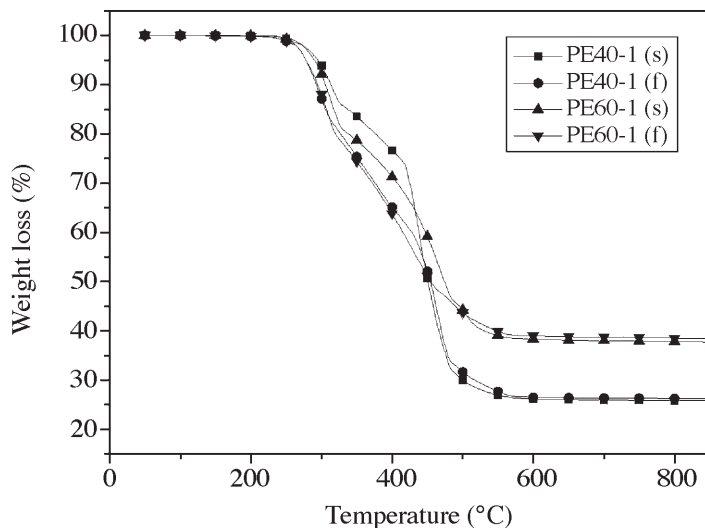


Figure 10. Thermogravimetric curves (TGA) for both foamed (f) and solid (s) samples with 40 wt.% and 60 wt.% of ATH

profiles of foamed and solid samples. To this purpose, **Figure 10** shows the thermogravimetric curves for 40 wt.% and 60 wt.% ATH content samples, both foamed and solid. No remarkable changes can be observed but for the slightly prematurely decomposition of foamed samples in both cases at the moment of the hydrocarbon chains decomposition, which could be due to trapped air inside the molten composite speeding up the thermo-oxidizing reactions.

3.4 Combustion Tests (LOI and Calorimeter Bomb)

Combustion behaviour of prepared LDPE foamed samples have been evaluated by means of LOI and calorimeter bomb tests. In **Figure 11**, the combustion heat values for solid and foamed samples are presented. As expected, these values decreased as loading levels are increased, since the combustible matrix reduces its content. This decrease has almost a linear trend, for both precursors (containing the blowing agent) and foams. It can be also observed that the values for the foamed samples are slightly higher, due to the contribution to the total combustion heat added to the material when the amount of blowing agent is substituted for the polymer. The heat of combustion of azodicarbonamide has been measured and it has a value of 5.86 MJ/kg.

On the other hand, the limiting oxygen index values for foamed samples are showed in **Figure 12** together with the reported LOI values for solid samples with similar ATH loading levels, as well as the char yield values obtained by means of the TGA experiments.

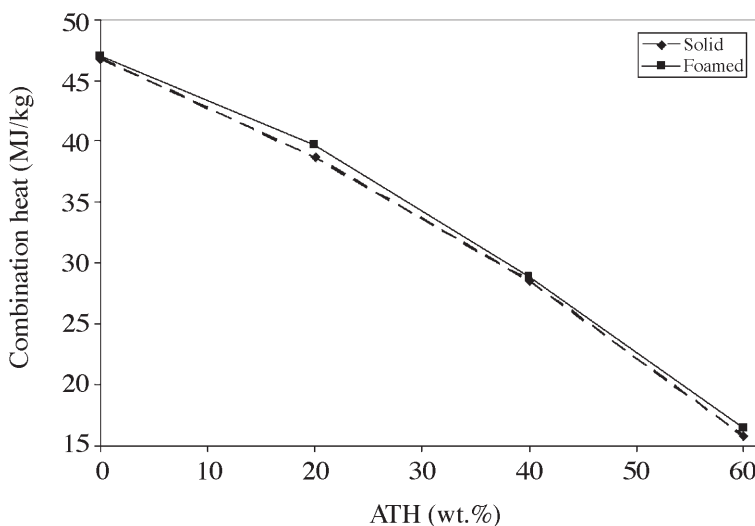


Figure 11. Combustion heat values for LDPE solid and foamed blends

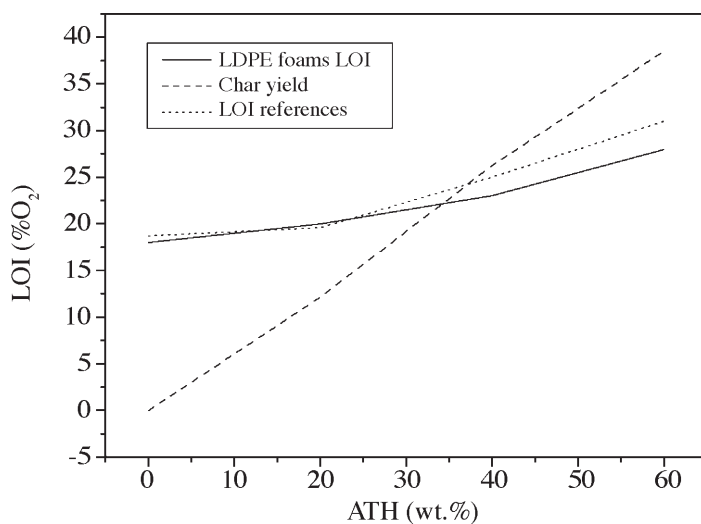


Figure 12. LOI and char yield values for LDPE blends

LOI values for foamed samples are similar to those reported for solid materials with similar chemical compositions^(27,28). Values for foamed samples are slightly smaller due to their cellular structure which promotes the transport of combustible gases inside the sample. This difference, almost insignificant for samples with a close-cell cellular structure, becomes higher for samples with interconnected cells, where this transport is promoted through the open channels of the cellular structure.

4. CONCLUSIONS

It has been demonstrated the feasibility of producing halogen-free flame retardant cellular materials based on LDPE with high filler loading, cell sizes below 100 microns and very similar fire behaviour than that of the solid from which the materials were produced. The improved compression moulding technique seems to be an adequate method to produce these light weight materials. Some interesting relationships between formulation and structure and between structure and properties have been found. The mechanical properties of materials incorporating the compatibilizing polymer are clearly improved. The amount of filler has an effect on the type of cellular structure, closed cells were observed for filler contents up to 50%, open cells were detected for filler contents of 60% or more. As expected the mechanical properties were reduced when foaming was carried out, interestingly the reduction in properties was

smaller when high filler loadings were used. The fire behaviour of the foamed samples was similar to that of solid materials with similar compositions. Bigger differences were found in the LOI measurements for those samples with an open-cell cellular structure, proving that a closed-cell cellular structure presents a better fire behaviour. Thermal stability proved as good for foams as for solid samples, finding a delay in the thermal decomposition as the loading levels are increased.

ACKNOWLEDGEMENTS

Financial assistance from the Local Government (Junta of Castile and Leon (Project VA047A07 and Excellence Group GR39), Spanish Ministry of Education and Science and FEDER program (project MAT 2006 1614-C03-01) is gratefully acknowledged.

REFERENCES

1. Troitzsch J.(Ed.), *Plastics flammability handbook: Principles, regulations, testing and approval*, Cincinnati, USA (2004).
2. Croce P.A., Bukowski R.W., *Fire Safety Journal*, **43** (2008), 234.
3. Troitzsch J.H., *Polymer Degradation and Stability*, **88** (2005), 146.
4. Grand A.F., Wilkie C.A., *Fire retardancy of polymeric materials*, USA (2000).
5. Mouritz A.P., Gibson A.G., *Fire properties of polymer composite materials*, Dordrecht (2006).
6. Wefers K., Misra C., *Oxides and hydroxides of aluminium*, Alcoa Laboratories, Alcoa technical paper n°19 (1987).
7. Okamoto K.T., *Microcellular processing*, Boston, USA (2003).
8. Bismark A., Powell R., *Polymer*, **47** (2006) 4513.
9. Velasco J.I., Rodríguez-Pérez M. A., *Polymer*, **48** (2007) 2098.
10. Sinha Ray S., Okamoto M., *Progress in Polymer Science*, **28** (2003) 1539.
11. Klempner D., Frish K.C., *Handbook of polymeric foams and foam technology*, NY, USA (1991).
12. Rodríguez-Pérez M.A, *Advances in Polymer Science*, **184** (2005) 87.
13. Chazeau L., Saint-Michel F., *Composites Science and Technology*, **66** (2006) 2709.

14. Hausmann K., Flaris V., *Polymer Composites*, **5** (1997) 113.
15. Mai K., Li Z., *Applied Polymer Science*, **80** (2001) 2617.
16. Hornsby P.R., Watson C.L., *Journal of Materials Science*, **30** (1995) 5347.
17. Hippi U., Mattila J., *Polymer*, **44** (2003) 1193.
18. Wang Z., Qu B., *Polymer Degradation and Stability*, **76** (2002) 125.
19. Chiang W., Ku Y., *Polymer Degradation and Stability*, **76** (2002) 281.
20. Rodríguez-Pérez M.A., Saja J.A., *Cellular Polymers*, **27** (2008) 327.
21. Rodríguez-Pérez M.A., Velasco J.I., Arencón D., Almanza O., de Saja J.A., *J. Appl. Polymer Sci*, **75** (2000) 156-166
22. Mills N.J., Rodríguez-Pérez, M.A., *Cellular Polymers*, **20** (2001) 79-100.
23. Rodríguez-Perez, M.A., Díez S., de Saja J.A., *Polymer Eng. & Sci*, **38** (1998) 831-837
24. Almanza O., Rodríguez-Perez M.A., de Saja J.A., *Polymer*, **42** (2001) 7117-7126
25. Rodríguez-Perez, M.A., de Saja J.A., *Cellular Polymers*, **18** (1999), 1-20.
26. Lee P.C., Park C.B., *Polymer Engineering and Science*, **45** 10 (2005) 1319.
27. Haurie L., Velasco J.I., Lopez Cuesta J.M., *Polymer Degradation and Stability*, **92** (2007) 1082.
28. Haurie L., Velasco J.I., Lopez Cuesta J.M., *Polymer Degradation and Stability*, **91** (2006) 989.